560 *Biochemistry* **2010,** *49,* 560–569
DOI: 10.1021/bi901717s

BIOCHEMISTRY
including biophysical chemistry & molecular biology
Article

The Structure of the Proline Utilization A Proline Dehydrogenase Domain Inactivated by *N*-Propargylglycine Provides Insight into Conformational Changes Induced by Substrate Binding and Flavin Reduction[†,‡]

Dhiraj Srivastava,[§] Weidong Zhu,[⊥] William H. Johnson Jr.,[@] Christian P. Whitman,[@] Donald F. Becker,[⊥] and John J. Tanner*[,§,∥]

[§]*Department of Chemistry, and* [∥]*Department of Biochemistry, University of Missouri, Columbia, Missouri 65211,* [⊥]*Department of Biochemistry, University of Nebraska, Lincoln, Nebraska 68588, and* [@]*Division of Medicinal Chemistry, College of Pharmacy, The University of Texas, Austin, Texas 78712*

Received October 5, 2009; Revised Manuscript Received December 7, 2009

ABSTRACT: Proline utilization A (PutA) from *Escherichia coli* is a flavoprotein that has mutually exclusive roles as a transcriptional repressor of the *put* regulon and a membrane-associated enzyme that catalyzes the oxidation of proline to glutamate. Previous studies have shown that the binding of proline in the proline dehydrogenase (PRODH) active site and subsequent reduction of the FAD trigger global conformational changes that enhance PutA−membrane affinity. These events cause PutA to switch from its repressor to its enzymatic role, but the mechanism by which this signal is propagated from the active site to the distal membrane-binding domain is largely unknown. Here, it is shown that *N*-propargylglycine irreversibly inactivates PutA by covalently linking the flavin N(5) atom to the ε-amino of Lys329. Furthermore, inactivation locks PutA into a conformation that may mimic the proline-reduced, membrane-associated form. The 2.15 Å resolution structure of the inactivated PRODH domain suggests that the initial events involved in broadcasting the reduced flavin state to the distal membrane-binding domain include major reorganization of the flavin ribityl chain, severe (35°) butterfly bending of the isoalloxazine ring, and disruption of an electrostatic network involving the flavin N(5) atom, Arg431, and Asp370. The structure also provides information about conformational changes associated with substrate binding. This analysis suggests that the active site is incompletely assembled in the absence of the substrate, and the binding of proline draws together conserved residues in helix 8 and the β1−αl loop to complete the active site.

The oxidative conversion of proline to glutamate requires the coupled activities of proline dehydrogenase (PRODH)[1] and Δ^1-pyrroline-5-carboxylate (P5C) dehydrogenase (P5CDH) (Scheme 1). In some bacteria, these activities are combined in a single polypeptide known as proline utilization A (PutA). The polypeptide chain lengths of PutAs exceed 1000 residues, with the PRODH and P5CDH domains appearing in the N-terminal and C-terminal halves of the protein, respectively (*1*, *2*). Some PutAs, including *Escherichia coli* PutA, also serve as transcriptional repressors of the *put* regulon, which comprises the divergently transcribed genes encoding PutA and the high-affinity Na^+/proline transporter, PutP, with an intervening 419 bp control DNA region (*1*, *3*). PutA represses transcription of *putA* and *putP* by recognizing, via an N-terminal ribbon−helix−helix domain, a consensus binding sequence that appears at five different locations in the *put* control DNA region. In the absence of proline, PutA occupies the five operator sites, thereby blocking transcription of the *put* genes (*3*). In the presence of proline, PutA associates with the membrane where it couples the oxidation of proline to P5C with reduction of the electron transport chain (Scheme 1). Following the nonenzymatic hydrolysis of P5C, the P5CDH domain catalyzes the NAD^+-dependent oxidation of γ-glutamate semialdehyde to glutamate (Scheme 1) (*4*−*6*). Thus, the association of PutA with the inner membrane not only is essential for efficient catalytic turnover but also increases the level of expression of *putA* and *putP* by preventing PutA from engaging its operator sites in the *put* control DNA region (*1*).

The process by which PutA is transformed from a DNA-bound repressor to a membrane-associated enzyme, known as functional switching, involves conformational changes triggered by proline binding and reduction of the flavin cofactor (*1*, *7*−*9*). Recently, conformational changes in the FAD were deduced from a structure of the dithionite-reduced *E. coli* PutA PRODH domain with hyposulfite bound in the proline binding site (*7*).

[†]This research was supported by National Institutes of Health (NIH) Grants GM065546 (to J.J.T.), GM061068 (to D.F.B.), and GM041239 (to C.P.W.). This research is a contribution of the University of Nebraska Agricultural Research Division, supported in part by funds provided through the Hatch Act. This publication was also made possible by NIH Grant P20 RR-017675-02 from the National Center for Research Resources.

[‡]Coordinates and structure factors have been deposited in the Protein Data Bank as entry 3ITG.

*To whom correspondence should be addressed. Telephone: (573) 884-1280. Fax: (573) 882-2754. E-mail: tannerjj@missouri.edu.

[1]Abbreviations: PutA, proline utilization A; PRODH, proline dehydrogenase; P5C, Δ^1-pyrroline-5-carboxylate; P5CDH, Δ^1-pyrroline-5-carboxylate dehydrogenase; PPG, *N*-propargylglycine; TtPRODH, *Thermus thermophilus* proline dehydrogenase; PutA86−630, protein corresponding to residues 86−630 of *E. coli* PutA; PutA86−669, protein corresponding to residues 86−669 of *E. coli* PutA; MES, 2-(*N*-morpholino)ethanesulfonic acid; THFA, L-tetrahydro-2-furoic acid; SDS, sodium dodecyl sulfate; HEPES-N, *N*-(2-hydroxyethyl)piperazine-*N*′-2-ethanesulfonic acid; rmsd, root-mean-square deviation; PDB, Protein Data Bank.

 Published on Web 12/08/2009

Scheme 1

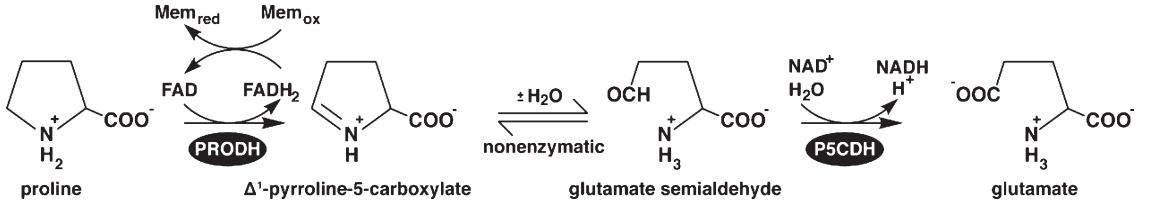

Upon reduction, the FAD was observed to adopt a new conformation characterized by a significant "butterfly" bend (22°) of the isoalloxazine ring and rotation of the 2′-OH group of the ribityl chain, resulting in formation of a new hydrogen bond between the 2′-OH group and the FAD N(1) atom (*7*). The 2′-OH group of the FAD was subsequently demonstrated to act as a redox-sensitive toggle switch that helps control association of PutA with the membrane (*7*).

A second key interaction involves the FAD N(5) atom and Arg431. Arg431 is strategically placed within hydrogen bonding distance of the flavin N(5) atom and is thus potentially able to sense changes in electron density across the N(1)−N(5) enediamine system attendant to FAD reduction. Indeed, mutation of Arg431 to Met, or replacement of FAD with 5-deaza-FAD, abrogated the ability of proline to activate binding of PutA to the membrane (*7*). Thus, Arg431 was proposed to have an important role in transmitting redox signals out of the FAD active site (*7*), although the dithionite-reduced enzyme structure did not indicate any movement of this residue.

The conformational changes in the FAD deduced from the structure of the dithionite-reduced PRODH domain (bending of the isoalloxazine ring and rotation of the 2′-OH group) presumably represent the initial step in transmission of the flavin redox status to a remote membrane-binding domain. Signal transmission likely involves Arg431, but other residues important for broadcasting the flavin redox state remain largely unknown.

Here, we have used mechanism-based inactivation of *E. coli* PutA by *N*-propargylglycine (PPG, **1** in Scheme 2) to elicit conformational changes similar to those involved in functional switching. This work was motivated by our recent study of the inactivation of PRODH from *Thermus thermophilus* (TtPRODH) by PPG (*10*). TtPRODH is a 307-residue monofunctional PRODH that is 27% identical in sequence to residues 235−569 of the 1320-residue *E. coli* PutA protein. The crystal structure of PPG-inactivated TtPRODH revealed a three-carbon link between the ε-amine of Lys99 and the N(5) atom of FAD. In one scenario, the mechanism of inactivation is initiated by the oxidation of PPG to *N*-propargyliminoglycine (**2** in Scheme 2) and concomitant reduction of the FAD. It is proposed that attack of **2** by N(5) of the reduced flavin, rearrangement of a putative allenic species (**3**) to an imminium intermediate (**4**), and nucleophilic attack by an active site lysine residue (Lys99) on the imminium intermediate lead to the covalent FAD−Lys99 adduct (**5**). As a result, the enzyme is, effectively, locked into the reduced state. Sequence alignments show that Lys99 is highly conserved among monofunctional PRODHs and PutAs, with Lys329 being the corresponding residue in *E. coli* PutA. Since PPG locks TtPRODH in the reduced state, we investigated the possibility of using PPG to stabilize the reduced conformation of PutA to facilitate examination of this important conformation. Results of these studies are described herein.

Scheme 2

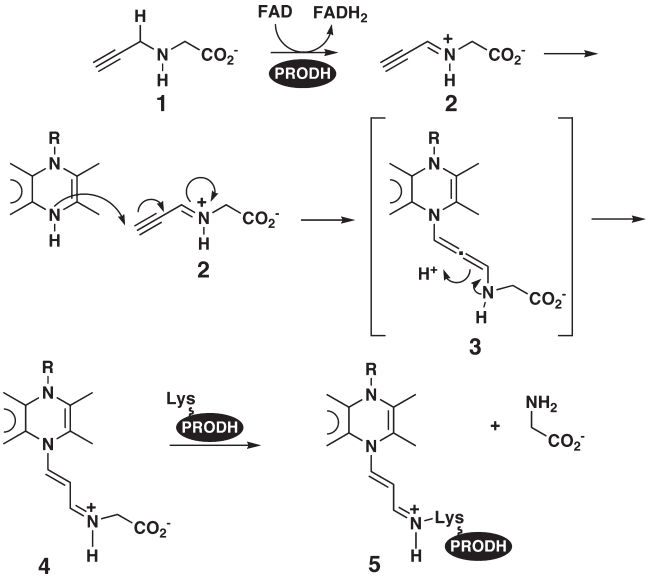

EXPERIMENTAL PROCEDURES

Materials. *N*-Propargylglycine (PPG) was synthesized as reported previously (*10*). *E. coli* polar lipid extracts, phosphatidylglycerol, and 1,2-dioleoyl-*sn*-glycero-3-ethylphosphocholine were purchased from Avanti Polar Lipids Inc. and used without purification. Full-length *E. coli* PutA and an *E. coli* PutA PRODH domain construct containing residues 86−630 (PutA86−630) were expressed and purified as previously reported (*8*, *11*, *12*). All chemicals and buffers were purchased from Fisher Scientific and Sigma-Aldrich, unless stated otherwise. All experiments used Nanopure water.

Crystallization. Crystallization experiments were performed with PutA86−630, which was purified by Ni-iminodiacetic acid chromatography and HiTrapQ anion exchange chromatography as described previously (*12*). After ion exchange, the protein was dialyzed into 50 mM Tris-HCl buffer, 50 mM NaCl, 0.5 mM EDTA, and 5% glycerol (pH 7.5). The sample was then concentrated to ∼12 mg/mL as estimated by the bicinchoninic acid method (Pierce kit). The protein was incubated with PPG in a ratio of 1 mg of enzyme/mg of PPG (∼560-fold molar excess of PPG) for at least 30 min at 4 °C. Crystallization experiments were performed at room temperature using the method of vapor diffusion. Initial crystallization conditions were identified using sitting drops and commercially available crystal screen kits. These experiments revealed promising crystals in solutions containing PEG 5000 monomethyl ether, ammonium sulfate, and 2-(*N*-morpholino)ethanesulfonic acid (MES) buffer. Following a few rounds of optimization, further improvement was obtained using an additive screen approach in which crystal screen reagents served as additive solutions. The base condition consisted of 26% (w/v) PEG 5000 monomethyl ether, 0.15 M

ammonium sulfate, and 0.1 M MES buffer (pH 5.8). Reservoir solutions were created by mixing the base condition and crystal screen reagent in a ratio of three parts base condition to one part crystal screen solution. The best results were obtained in hanging drops using Index reagent 82 as the additive [0.2 M $MgCl_2$, 0.1 M Bis-Tris buffer, and 25% (w/v) PEG 3350 (pH 5.5)]. In preparation for low-temperature data collection, the crystals were soaked in 22% (w/v) PEG 5000 monomethyl ether, 112.5 mM ammonium sulfate, 50 mM $MgCl_2$, 9% (w/v) PEG 3350, 100 mM MES buffer (pH 5.8), and 20% (v/v) PEG 200, picked up with Hampton mounting loops, and plunged into liquid nitrogen.

X-ray Diffraction Data Collection, Processing, and Refinement. Diffraction data were collected at beamline 4.2.2 of the Advanced Light Source. The data set used for structure determination and refinement consisted of 200 frames collected with an oscillation width of 0.5° per frame and a detector distance of 160 mm. The data were integrated with MOSFLM (*13*) through the iMosflm graphical interface and scaled to 2.15 Å resolution with SCALA (*14*) using the CCP4i interface (*15*). The space group is $I2_12_12_1$ with the following unit cell dimensions: a = 127.5 Å, b = 133.4 Å, and c = 133.6 Å. There are two molecules in the asymmetric unit, which implies a solvent content of 47% and a V_m of 2.3 $Å^3$/Da (*16*). Data processing statistics are listed in Table 1. We note that this crystal form differs from the one used in previous crystallographic studies of the *E. coli* PutA PRODH domain, which is in space group *I*222 with one molecule in the asymmetric unit and the following unit cell dimensions: a = 73 Å, b = 141 Å, and c = 146 Å (*7*, *12*, *17*−*19*).

The structure was determined using molecular replacement as implemented in MOLREP (*20*). The search model was derived from the coordinates of the *E. coli* PutA PRODH domain complexed with the inhibitor L-tetrahydro-2-furoic acid [THFA; PDB entry 1TIW (*19*)]. The structure was refined with PHENIX (*21*). Model building was performed with Coot (*22*).

The final model includes two protein chains, a covalently modified FAD cofactor bound to each protein chain, and 241 water molecules. Each protein chain includes residues 87−137, 258−555, and 561−610. As with all other structures of the *E. coli* PutA PRODH domain (*7*, *12*, *18*, *19*), electron density for residues 138−257 is weak, and thus, these residues were not modeled. As described in Results, inactivation by PPG induces substantial disorder in α8 (residues 545−562). Because of the weak electron density in this region of the structure, residues 549−555 were modeled as polyalanine and residues 556−660 were not modeled. The two protein chains have identical conformations within experimental error (root-mean-square deviation of 0.12 Å for C_α atoms). Likewise, the active site structures of the two chains are identical. Refinement statistics are listed in Table 1.

Spectroscopic and Kinetic Characterization of the Inactivation of Full-Length E. coli PutA. Spectral changes associated with inactivation of full-length PutA by PPG were monitored by a Cary-100 spectrophotometer using the wavelength range of 300−600 nm at 25 °C. The absorbance spectrum of oxidized PutA was measured in a quartz cuvette at 10 μM in 50 mM potassium phosphate buffer (pH 7.5) with 10% glycerol. A quartz cuvette with buffer served as the reference. A fresh 50 mM stock solution of PPG was added to the cuvette at a final PPG concentration of 500 μM. The solution was then briefly mixed via cuvette inversion. Spectra were recorded immediately after the cuvette was returned to the cuvette holder and at subsequent 20 s intervals for 0−3 min, 30 s intervals for 3−10 min, 60 s intervals for 10−60 min, and 120 s intervals for 60−90 min. After PPG treatment, the extent of inactivation exceeded 95%. PPG-inactivated PutA was denatured via addition of sodium dodecyl sulfate (SDS) to a final concentration of 0.2% [in 50 mM sodium phosphate buffer and 10% glycerol (pH 7.5)] as described elsewhere (*23*), and the resulting flavin spectrum was recorded. Free FAD was then separated from denatured PutA by centrifugation using a 10 kDa cutoff membrane. The molar extinction coefficients for the flavin compounds with maximum absorbance at 378 and 397 nm were estimated using the flavin concentration determined for native PutA (ε_{451} = 12700 M^{-1} cm^{-1}) prior to inactivation.

Table 1: Data Collection and Refinement Statistics[a]

space group	$I2_12_12_1$
unit cell lengths (Å)	a = 127.5, b = 133.4, c = 133.6
wavelength (Å)	1.0000
diffraction resolution (Å)	31.5−2.15 (2.25−2.15)
no. of observations	243987
no. of unique reflections	60418
redundancy	4.0 (3.3)
completeness (%)	97.9 (98.9)
$R_{merge}(I)$	0.094 (0.489)
$R_{pim}(I)$	0.053 (0.303)
average I/σ	10.3 (3.3)
Wilson B-factor ($Å^2$)	26
no. of protein chains	2
no. of atoms	6480
no. of protein residues	800
no. of FAD atoms	106
no. of water molecules	241
R_{cryst}[b]	0.193 (0.250)
R_{free}[b]	0.234 (0.292)
rmsd[c]	
bond lengths (Å)	0.006
bond angles (deg)	0.98
Ramachandran plot[d]	
favored (%)	98.1
allowed (%)	1.9
outliers (%)	0.0
average B-factor ($Å^2$)	
protein	34
FAD	26
modified Lys329	27
water	31
coordinate error (Å)[e]	0.52
PDB entry	3ITG

[a]Values for the outer resolution shell of data are given in parentheses. [b]A 5% random test set. [c]Compared to the Engh and Huber parameters (*30*). [d]The Ramachandran plot was generated with RAMPAGE (*31*). [e]Maximum likelihood-based coordinate error reported by PHENIX.

The kinetic parameters for PRODH activity of full-length PutA were determined as described previously for TtPRODH (*10*). Accordingly, a fresh 50 mM stock solution of PPG dissolved in 50 mM potassium phosphate buffer (pH 7.5) and 10% glycerol was prepared. *E. coli* PutA (5 μM) was incubated at 25 °C with PPG at concentrations of 0.25, 0.5, 0.75, 1.0, and 2.5 mM. Aliquots were removed at 15 min intervals over a period of 120 min and assayed at 25 °C using a previously described PRODH assay based on the reduction of dichlorophenolindophenol with L-proline (80 mM) as the substrate. Inactivation parameters were estimated using the standard method of extracting half-lives from plots of the natural logarithm of activity versus time and making a Kitz and Wilson replot (*24*, *25*).

Conformational Changes of Full-Length PutA Accompanied by N-Propargylglycine Inactivation. Limited proteolysis

of full-length PutA by chymotrypsin was performed as previously described with the following modifications (*26*). In all digests, PutA was preincubated with 5 mM proline or 5 mM THFA, for 5 min prior to addition of chymotrypsin except for PPG, which was incubated with PutA for 30 min. Proline and THFA were dissolved in 50 mM potassium phosphate buffer (pH 7.5). PutA (1 mg/mL) was then digested with chymotrypsin (10 μg/mL) for 1 h at 25 °C in 50 mM potassium phosphate buffer (pH 7.5) containing 10% glycerol. The reactions were stopped via addition of phenylmethanesulfonyl fluoride (final concentration of 2 mM) and hot SDS−PAGE sample buffer at a 1:2 (v/v) ratio of SDS buffer to sample. The samples (7.5 μg each) were analyzed by SDS−PAGE using 8% acrylamide separating gels. As a control, oxidized PutA (2.5 μg) without digestion was also run on the gel. Gels were visualized after Coomassie Blue G-250 staining and imaged using a Bio-Rad Gel Doc 2000 System. The molecular weight marker was the Precision Dual Color reagent (Bio-Rad).

Assays of Full-Length PutA Binding to E. coli Polar Lipids. The binding buffer used in these experiments consisted of 10 mM *N*-(2-hydroxyethyl)piperazine-*N*′-2-ethanesulfonic acid containing 150 mM NaCl (pH 7.4) (HEPES-N buffer). *E. coli* polar lipid vesicles were prepared as previously described using a LiposoFast microextruder with a 100 nm polycarbonate filter at a final concentration of 5 mg/mL (*8*). After preincubation of full-length PutA (0.25 mg/mL) with proline (5 mM, 5 min), THFA (5 mM, 5 min), or PPG (5 mM, 30 min) at 25 °C in 150 mM HEPES-N buffer, the freshly prepared *E. coli* polar lipid vesicles were added to the reaction mixtures to a final concentration of 0.8 mg/mL and incubated at room temperature for 1 h with slow rotation. The lipid-bound fraction was then separated from the solution phase using an air-driven ultracentrifuge (Airfuge, Beckman) at the maximum speed as previously described (*27*). The supernatant (soluble phase) was removed and denatured with SDS sample buffer and labeled as soluble fractions. The lipid pellet was resuspended in an equal volume of HEPES-N buffer, denatured with SDS sample buffer, and labeled as the lipid fraction. Nonspecific sedimentation of the PutA proteins was not observed in the absence of the lipids. All the soluble and lipid fractions were analyzed with 10% SDS−polyacrylamide gels, which were stained with Coomassie Blue G-250. Quantitative analysis of gels was performed with a Bio-Rad Gel Doc 2000 System.

RESULTS

Spectral Analysis of the Inactivation of Full-Length E. coli PutA by PPG. Similar to that observed with TtPRODH, PPG inactivates full-length *E. coli* PutA with a concomitant spectral change (Figure 1A). The absorption spectrum of PutA-bound FAD decreases at 451 nm after the addition of PPG. Coinciding with the decrease at 451 nm is a dramatic increase in absorbance at 378 nm ($\varepsilon \sim 20800$ M^{-1} cm^{-1}). The decrease at 451 nm indicates that the FAD is fully reduced, similar to reduction of the flavin by sodium dithionite or the substrate proline. The significant increase at 378 nm, which is not observed with proline or dithionite, suggests a new reduced flavin species is formed. The new species is most likely the Lys329−FAD covalent adduct shown in Scheme 2 (**5**). Formation of this adduct was confirmed by X-ray crystallography (vide infra).

The covalently modified flavin could be separated from the inactivated enzyme by treating PPG-inactivated PutA with a 0.2% SDS solution and isolating the flavin component by membrane filtration. The isolated flavin exhibits a strong absorbance

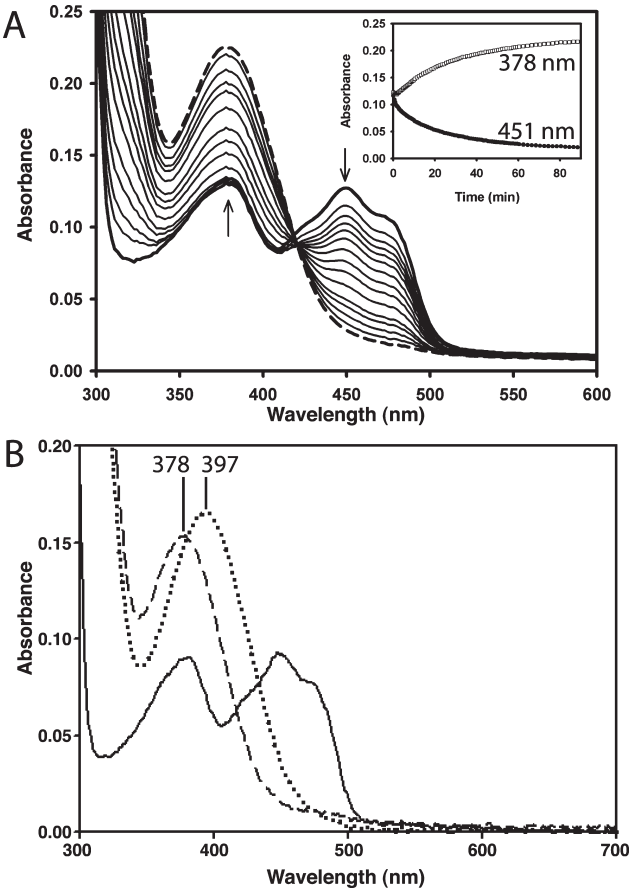

FIGURE 1: Spectroscopic analysis of the inactivation of full-length *E. coli* PutA by PPG. (A) Flavin spectral changes of *E. coli* PutA induced by inactivation by PPG. The spectrum of oxidized PutA is represented as the thick curve and has maxima (λ) at 451 and 378 nm. Spectra were acquired immediately after addition of 500 μM PPG and were continually collected for up to 90 min as described in Experimental Procedures. For the sake of clarity, only 14 spectra are shown, with the dashed curve indicating the last spectrum. Note that the maximum at λ = 451 nm disappears (decreases) and a new maximum centered at λ = 378 nm appears (increases) as time advances. The inset shows the absorbance recorded at 451 nm (●) and 378 nm (○) during the 90 min inactivation process. (B) Denaturation of PPG-inactivated PutA. Spectra are as follows: PutA (7.35 μM) before inactivation (—), PutA inactivated with 500 μM PPG for 90 min (---), and the flavin species isolated after treatment of PPG-inactivated PutA with 0.2% SDS (···).

maximum at 397 nm ($\varepsilon \sim 22750$ M^{-1} cm^{-1}) [Figure 1B (···)], which is similar to the spectrum of PPG-inactivated PutA [Figure 1B (---)] and distinctly different from the spectrum of oxidized PutA [Figure 1B (—)]. This result suggests that the isolated flavin is covalently modified, albeit separated from the enzyme. Presumably, the Schiff base in **5** of Scheme 3 undergoes hydrolysis to produce **6** of Scheme 3 and the free enzyme as a result of treatment with SDS buffer.

Kinetic Analysis of the Inactivation of Full-Length E. coli PutA by PPG. The inactivation of full-length PutA by PPG was monitored in a time- and concentration-dependent manner, as shown in Figure 2. Inactivation profiles of PutA with five different PPG concentrations were used to estimate inactivation parameters. The standard method of extracting half-lives from plots of the natural logarithm of activity versus time was used to construct a Kitz and Wilson replot (Figure 2, inset). Note that the Kitz and Wilson replot intersects the ordinate above the origin, which suggests that inactivation proceeds with saturation, i.e.,

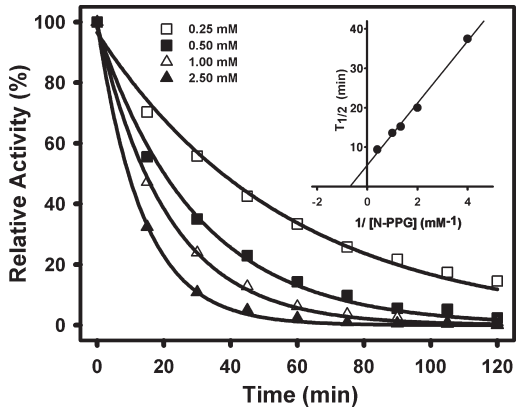

FIGURE 2: Kinetics of PutA inactivation by PPG at 25 °C using a dichlorophenolindophenol-based activity assay. The percent activity remaining after incubation with PPG is plotted as a function of time for four inactivator concentrations (from 0.25 to 2.5 mM). The inset shows the replot of the half-life of inactivation as a function of the reciprocal concentration of PPG. The following inactivation parameters were obtained from fitting: $k_{inact} = 0.13 \pm 0.05$ min^{-1}, and $K_I = 1.5 \pm 0.2$ mM.

Scheme 3

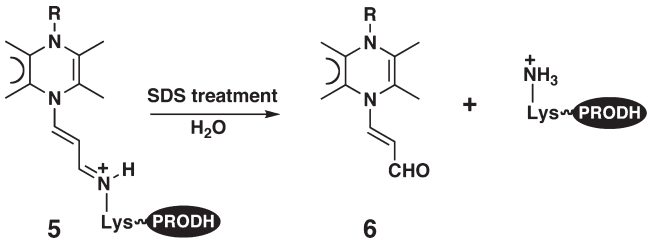

that a dissociable complex forms prior to inactivation (*25*). This complex of enzyme and PPG is analogous to the binding of enzyme and substrate in the E·S complex. The estimated values of k_{inact} and K_I are 0.13 min^{-1} and 1.5 mM, respectively.

Structural Characterization of the Enzyme−FAD Adduct. The structure of an *E. coli* PutA PRODH domain construct (PutA86−630) inactivated by PPG was determined to confirm formation of a Lys−FAD covalent adduct, i.e., **5** in Scheme 2. The structure was determined at 2.15 Å resolution using molecular replacement (Table 1). As expected, the enzyme displays the distorted $(\beta\alpha)_8$ barrel fold characteristic of the PRODH family (Figure 3). The FAD cofactor is bound at the C-termini of the strands of the barrel, with the *re* face of the isoalloxazine packed against strands 4−6 of the barrel.

Electron density maps clearly indicated that the flavin is covalently modified by PPG (Figure 4). Inactivation with PPG results in covalent attachment of Lys329 to the flavin N(5) atom via a three-carbon linkage (Figure 4A). Also, the flavin isoalloxazine ring is distinctly nonplanar, being bent by ~35° around the N(5)−N(10) axis (Figure 4B). Such deviations from planarity are termed butterfly conformations and are associated with reduced states of the flavin. We note that the isoalloxazine ring of the dithionite-reduced enzyme also exhibits a butterfly conformation (bend angle of 22°), and the isoalloxazine ring of the oxidized enzyme is planar. Both the covalent attachment of an active site lysine residue to the flavin N(5) atom and the butterfly conformation were observed in PPG-inactivated TtPRODH (*10*).

Limited Proteolysis Studies of Full-Length E. coli PutA. As reported previously, oxidized, reduced, and inhibited forms of

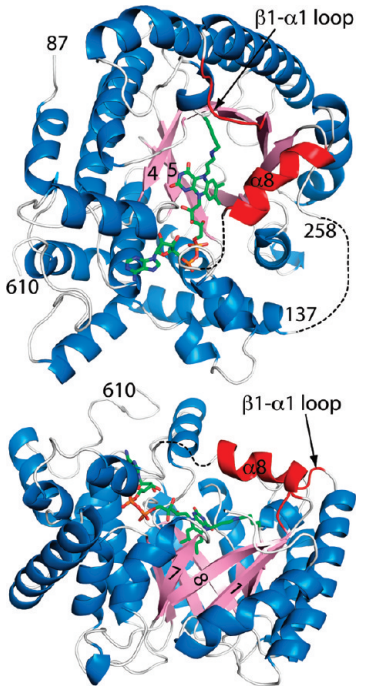

FIGURE 3: Two views of PPG-inactivated PutA86−630. Strands and helices are colored pink and blue, respectively. The dashed curves denote disordered segments of the polypeptide chain. The covalent FAD−Lys329 adduct is colored green. Red coloring denotes regions displaying large conformational differences from other PutA PRODH domain structures (i.e., α8 and the β1−α1 loop).

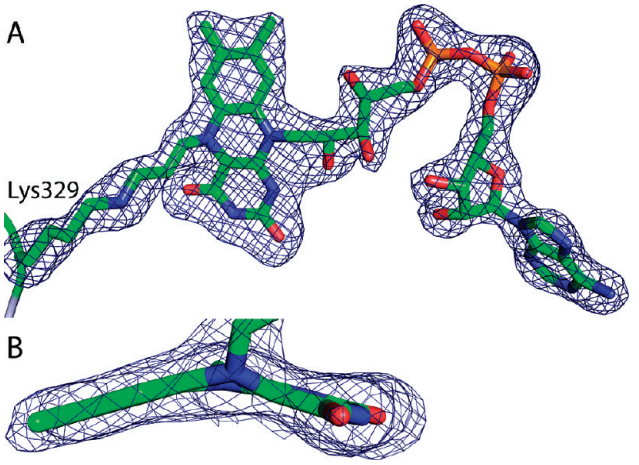

FIGURE 4: Electron density maps showing the (A) overall FAD conformation and covalent attachment to Lys329 and (B) curvature of the isoalloxazine ring. The cage represents a simulated annealing σ_A-weighted $F_o - F_c$ map contoured at 3σ. Prior to calculation of the map, the FAD and side chain of Lys329 were omitted, and simulated annealing refinement was performed with PHENIX.

full-length *E. coli* PutA have unique proteolytic fingerprints (*26*). Therefore, the PPG-inactivated enzyme was also subjected to limited proteolysis using chymotrypsin. As shown in Figure 5, oxidized PutA displays major proteolysis bands at 135 and 111 kDa, whereas the proline-reduced enzyme displays bands at 119 and 111 kDa. PutA inhibited by the nonreducing proline analogue THFA exhibits a predominant band at ~90 kDa. These results are in excellent agreement with previous studies (*26*). PutA inactivated with PPG displays prominent bands at 119 and 111 kDa, a pattern similar to that observed with proline-reduced PutA. These results suggest that the global structure of the PPG-inactivated

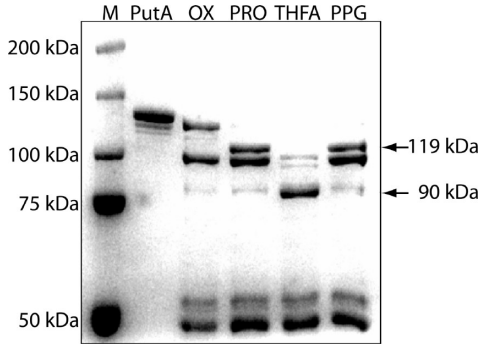

FIGURE 5: Conformational changes during PutA inactivation by PPG detected by limited proteolysis. Purified PutA (1 mg/mL) was incubated for 5 min each with proline (5 mM) or THFA (5 mM) or for 30 min with PPG (5 mM) in 50 mM potassium phosphate (pH 7.5) followed by digestion with chymotrypsin (10 μg/mL) for 1 h at 23 °C. The reactions were quenched with phenylmethanesulfonyl fluoride and hot SDS sample buffer after 1 h. After complete denaturation in SDS buffer, 7.5 μg of each digestion was loaded onto an 8% polyacrylamide denaturing gel for analysis. As a control, undigested ligand-free PutA was also loaded (2.5 μg). The gel was stained with Coomassie Blue to visualize the major products. A molecular mass marker (M) was loaded in the first lane.

enzyme resembles that of the proline-reduced enzyme, and that PPG and proline trigger similar conformational changes in PutA.

Lipid Associations of PPG-Inactivated Full-Length E. coli PutA. Physical lipid binding assays were performed in which full-length PutA was incubated with *E. coli* polar lipid vesicles, and the soluble and lipid-bound protein fractions were separated by centrifugation. Results of this assay for the oxidized, proline-reduced, THFA-bound, and PPG-inactivated forms of PutA are shown in Figure 6. As expected, oxidized PutA is detected almost entirely in the soluble fraction, indicating that it does not associate with the lipid vesicles (Figure 6A). The corresponding soluble/lipid partitioning ratio is 98/2 (Figure 6B). In contrast, proline-reduced PutA exhibits a soluble/lipid distribution of 35/65, indicating that reduction of the FAD by the substrate induces a dramatic increase in the level of lipid binding. THFA also strengthens PutA−lipid associations relative to the inhibitor-free, oxidized enzyme, but to a lesser extent than proline. The soluble/lipid ratio for THFA-bound PutA is 57/43. These results are consistent with surface plasmon resonance studies (*8*) showing that oxidized PutA displays no binding to *E. coli* polar lipid vesicles, proline induces very tight binding (K_D < 0.01 nM), and THFA stimulates moderately strong binding (K_D = 34 nM). PPG-inactivated PutA displays a soluble/lipid ratio of 34/66, which is comparable to that of the proline-reduced enzyme (Figure 6B). These results suggest that PPG causes PutA−lipid associations that are similar to those induced by proline.

Comparison to Other PRODH Structures. Since PPG mimics the effects of proline on PutA conformation and PutA lipid binding, the structure of PPG-inactivated PutA86−630 was compared to other PutA PRODH structures to gain insight into conformational changes involved in functional switching. Also, because this structure is the only one of a PutA PRODH domain without a ligand occupying the proline binding site, such a comparison potentially provides clues about conformational changes associated with substrate binding. The relevant structures in the PDB are those of oxidized PutA86−669 (residues 86−669 of *E. coli* PutA) in a complex with the proline analogue THFA (PDB entry 1TIW) and dithionite-reduced PutA86−669 in a complex with hyposulfite (PDB entry 2FZM).

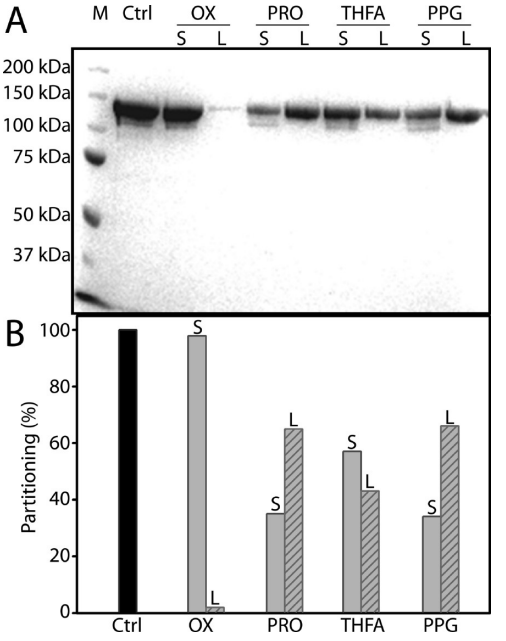

FIGURE 6: Physical binding of PPG-inactivated PutA to *E. coli* polar lipids. (A) PutA (0.25 mg/mL) was preincubated with HEPES-N buffer with 5 mM proline, 5 mM THFA, or 5 mM PPG for 5, 5, or 30 min, respectively, and then incubated with freshly prepared *E. coli* polar lipids (0.8 mg/mL) for 1 h at room temperature. The soluble and lipid fractions were then separated by Air-fuge ultracentrifugation, denatured with SDS buffer, and analyzed via SDS−PAGE. As a control, an equal amount of denatured PutA without treatment was also loaded. (B) Quantitative analysis of PutA bands for the soluble (gray bars) and lipid (gray hatched bars) fractions normalized as a percentage of total PutA using a Bio-Rad 2000 system.

The structure of PPG-inactivated PutA86−630 reveals a new conformation for the FAD ribityl chain of PutAs (Figure 7A). The 2′-OH group is tucked below the pyrimidine ring and forms hydrogen bonds with the FAD N(1) atom and Gly435. The 3′-OH group is rotated 66° from the 2′-OH group and forms a hydrogen bond with the FAD ribose. The 4′-OH group is oriented *trans* to the 3′-OH group and forms a hydrogen bond with a conserved water molecule buried on the *re* side of the FAD. We note that this ribityl conformation is very similar to that of the FAD in oxidized and PPG-inactivated TtPRODH.

The ribityl hydroxyl groups are arrayed much differently in other structures of the PutA PRODH domain (Figure 7B,C). In the THFA complex, the 2′-OH and 3′-OH groups point into the proline binding site where they form hydrogen bonds with Arg556 and Glu559, respectively (Figure 7B). Both residues are conserved in PutAs and are located on helix α8. As described below, these critical residues are disordered in the PPG-inactivated enzyme. The 4′-OH group of the THFA complex is *trans* to the 3′-OH group and forms hydrogen bonds with Gly435 and the FAD ribose. The ribityl chain of the dithionite-reduced enzyme is identical to that of the THFA complex, except that the 2′-OH group sits below the flavin N(1) atom, as in the PPG-inactivated enzyme (Figure 7C).

Significant differences are also observed in the protein components of the active site. Since the THFA complex and the dithionite-reduced enzyme structures have identical protein conformations, we will restrict the following analysis to a comparison with the THFA complex.

The PPG-inactivated enzyme differs from the other PutA PRODH structures in the conformations of two residues near the FAD N(5) atom, Arg431 and Asp370 (Figure 8). In the

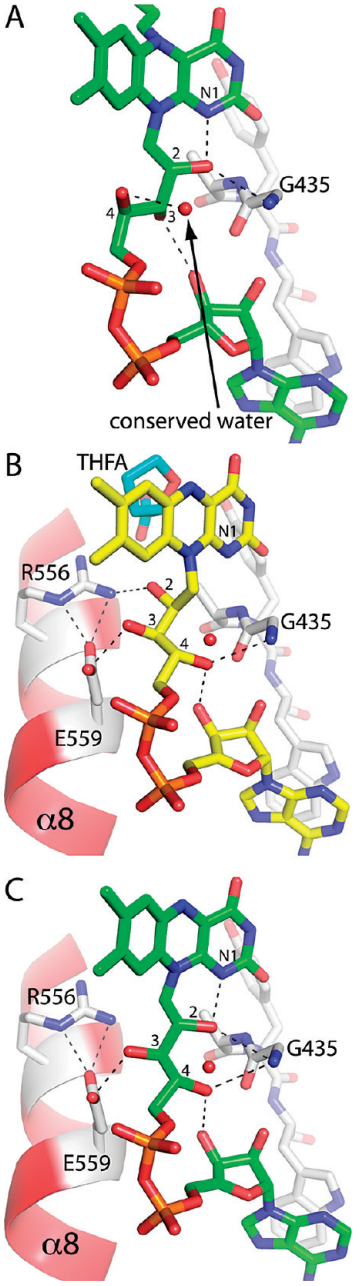

FIGURE 7: FAD conformations observed in three crystal structures of the *E. coli* PutA PRODH domain: (A) PPG-inactivated PutA86−630, (B) oxidized PutA86−669 in a complex with THFA (cyan), and (C) dithionite-reduced PutA86−669. Helix α8 is colored red for the latter two enzymes; this helix is disordered in PPG-inactivated PutA86−630. Note that the reduced flavins are colored green (A and C), whereas the oxidized flavin is colored yellow (A). The three flavins are oriented such that the AMP moieties are superimposed.

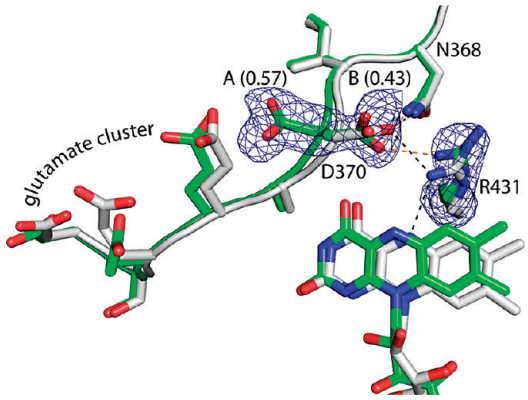

FIGURE 8: Close-up view of structural differences between PPG-inactivated PutA86−630 (green) and PutA86−669 in a complex with THFA (white), highlighting the movements of Arg431 and Asp370. The occupancy values for the two conformations of Asp370 in the inactivated enzyme are given in parentheses. Orange dashed lines represent hydrogen bonds in the PPG-inactivated enzyme. Black dashed lines represent hydrogen bonds in the THFA complex. The cage represents a simulated annealing σ_A-weighted $F_o - F_c$ map contoured at 3σ. Prior to calculation of the map, the side chains of Asp370 and Arg431 were omitted, and simulated annealing refinement was performed with PHENIX.

THFA complex, Arg431 donates a hydrogen bond to the FAD N(5) atom (3.1 Å) and forms an ion pair with Asp370 (also 3.1 Å). In the PPG-inactivated enzyme, the Arg431−N(5) distance has increased to 4.2 Å, indicating disruption of this key interaction. Furthermore, electron density maps indicated that Asp370 occupies two conformations in the PPG-inactivated enzyme (Figure 8). One of these conformations corresponds to the one observed in the THFA complex (labeled B in Figure 8). In the other conformation (labeled A in Figure 8), Asp370 is rotated 180° away from Arg431 and toward a cluster of glutamate residues located on the surface of the protein (residues 372, 373, and 375). When Asp370 is in conformation A, the ion pair with Arg431 and hydrogen bond with Asn368 are not formed.

Profound structural differences are also observed in two regions important for proline binding, α8 (residues 545−562) and the loop connecting β1 to α1 (residues 287−292). As shown in Figure 9, α8 is shifted by 3 Å away from the isoalloxazine ring and substantially disordered in the inactivated enzyme. Electron density in the region expected for α8 was quite weak, and although the density allowed the modeling of residues 545−555 in an α-helical conformation, residues 549−555 were modeled as polyalanine due to a complete absence of density for the side chains. Furthermore, density for residues 556−660 was not apparent, and these residues were omitted entirely from the final model (dashed curve in Figure 9). The conformation of the β1−α1 loop is also quite different in the inactivated enzyme. In the PPG-inactivated enzyme, this loop is shifted away from the active site by 4 Å, and the side chain of Glu289 is disordered (Figure 9). As a result, the Glu289−Arg555 ion pair, which is observed in all other PutA PRODH structures, is broken in the PPG-inactivated enzyme.

Interestingly, the conformations of α8 and the β1−α1 loop are reminiscent of those in the structure of oxidized TtPRODH [PDB entry 2G37 (*28*)], the only other PRODH structure without a ligand bound in the proline binding site. A comparison of these two ligand-free enzymes with the PutA86−669·THFA complex is shown in Figure 10. As in PPG-inactivated PutA86−630, α8 of TtPRODH is shifted away from the isoalloxazine ring, the β1−α1 loop is withdrawn from the active site, and the conserved ion pair (Glu65−Arg288) is broken. Consequently, the active sites of the ligand-free enzymes are more open than in the PutA86−669·THFA complex.

DISCUSSION

Mechanism-Based Inactivation of PRODH. Mechanism-based inactivation of PRODH was first reported in 1993, but this area of research is nascent nonetheless. In the first study, Trisch et al. found that 4-methylene-L-proline decreased the PRODH activity of rat mitochondrial extracts (*29*). This area of research

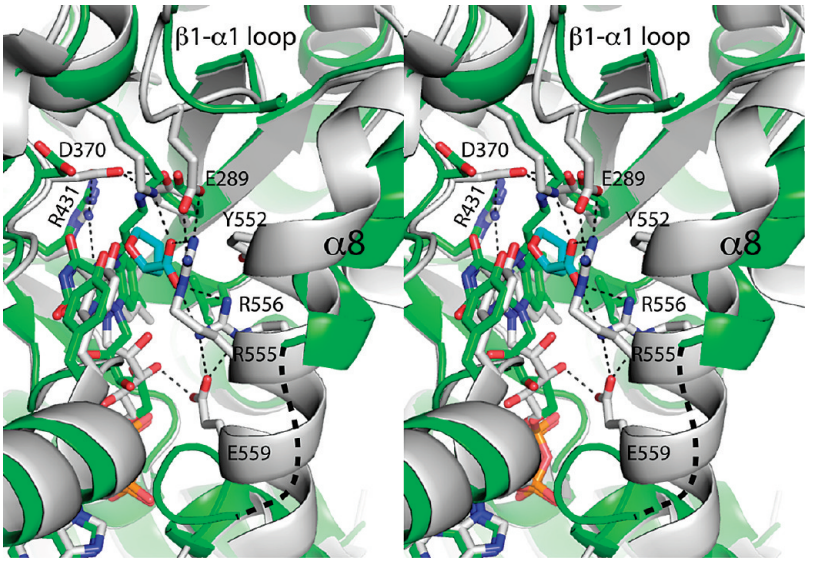

FIGURE 9: Stereographic view of a superposition of the active sites of PPG-inactivated PutA86−630 (green) and PutA86−669 in a complex with THFA (white). The THFA ligand is colored cyan. The thin dashed lines indicate hydrogen bonds of the THFA complex. The thick dashed curve denotes the disordered section of α8 of the PPG-inactivated enzyme. For the sake of clarity, conformation B of Asp370 of the inactivated enzyme has been omitted.

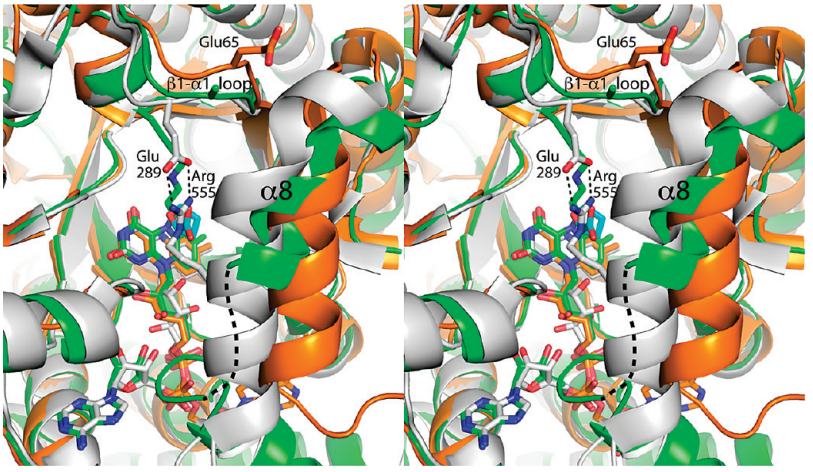

FIGURE 10: Stereographic view of a comparison of PPG-inactivated PutA86−630 (green), PutA86−669 in a complex with THFA (white), and TtPRODH (orange). The THFA ligand is colored cyan. The thin dashed lines indicate the Arg555−Glu289 ion pair observed in the THFA complex. Note that Glu289 is disordered in the PPG-inactivated enzyme (modeled as Ala), and the corresponding residue of TtPRODH (Glu65) points out of the active site and into the solvent. The thick dashed curve denotes the disordered section of α8 of the PPG-inactivated enzyme.

lay dormant until our report of the inactivation of TtPRODH by PPG in 2008 (*10*). In the study presented here, we have further shown that PPG is also an inactivator of the PRODH domain within PutA (Figure 2). The kinetic constants for PutA inactivation (k_{inact} = 0.13 min^{-1}, and K_I = 1.5 mM) are similar to those of TtPRODH (k_{inact} = 0.43 min^{-1}, and K_I = 0.8 mM). Furthermore, as with TtPRODH, a dissociable complex is likely formed between PutA and PPG before inactivation of the enzyme. The structures of the PPG-inactivated active sites of PutA and TtPRODH are also similar. In both cases, the flavin is highly bent and covalently attached to an active site lysine by a three-carbon linkage. These similarities suggest that PutA and TtPRODH share a common mechanism of inactivation by PPG. The fact that PPG inactivates both monofunctional PRODH and PutA suggests that it could be a broad-based inactivator of the PRODH family. A critical test of this idea will be whether PPG inactivates monofunctional eukaryotic PRODHs.

Insight into Conformational Changes of PutA Induced by Substrate Binding and Flavin Reduction. PPG-inactivated *E. coli* PutA exhibits spectral features, proteolysis patterns, and lipid binding properties similar to those of proline-reduced PutA, implying that PPG and proline induce analogous conformational changes in PutA. Therefore, we suggest that the structure of PPG-inactivated PutA86−630 is relevant for understanding the conformational changes involved in functional switching of PutA. In particular, the structure may provide insight into the changes occurring in the vicinity of the flavin that help to broadcast the reduced flavin redox state to the distal membrane-binding domain.

The PPG-inactivated enzyme structure may also be relevant for understanding conformational changes associated with substrate binding or, equivalently, product release, because it is the first one of a PutA PRODH domain without a ligand in the proline binding site. All structures of the oxidized PutA PRODH domain have a competitive inhibitor, such as THFA, L-lactate, or acetate, bound in the active site. These structures are good models of the Michaelis complex between the oxidized enzyme and the substrate, and they show that proline is completely buried in the

active site, implying that protein conformational changes must accompany substrate binding and product release. The structure of the dithionite-reduced enzyme did not provide insight into such conformational changes because a hyposulfite ion, an oxidation product of dithionite, occupies the proline site (*7*). Because the structure of the empty active site has proven to be elusive, the nature of the conformational changes attendant to substrate binding and product release is currently unknown.

Our analysis of the available structures indicates four regions of interest with regard to conformational changes associated with flavin reduction and substrate binding: the FAD cofactor, residues near the FAD N(5) atom (Arg431 and Asp370), α8, and the β1−αl loop.

Involvement of the FAD ribityl chain in functional switching is consistent with previous biochemical and structural studies. Membrane binding studies with mutant PutA proteins and PutA reconstituted with 2-deoxy-FAD showed that the 2′-OH group acts as a redox-sensitive switch that controls membrane association (*7*). The structures of the PPG-inactivated and dithionite-reduced enzymes indicate that reduction of the flavin induces a 90° rotation in this group. Additionally, the former structure reveals a more substantial reorganization of the ribityl chain involving all three hydroxyl groups and a larger distortion of the isoalloxazine ring (butterfly bend). Although it seems clear that the bending of the isoalloxazine ring and rotation of the 2′-OH group are associated with functional switching, whether the conformational changes of the 3′-OH and 4′-OH groups are consequences of the reduced flavin state or empty proline binding site remains to be determined.

It should be noted that the experimental details of crystal preparation might explain some of the differences between the flavin conformations observed in the structures of the PPG-inactivated and dithionite-reduced enzymes. The crystal used to determine the former structure was grown from inactivated enzyme, and thus, conformational changes induced by inactivation were allowed to proceed in solution. In contrast, the latter structure was determined from an oxidized crystal that was soaked in dithionite prior to being freeze-trapped in liquid nitrogen. In this case, the preformed crystal lattice likely prohibited extensive conformational changes. Furthermore, the use of a high dithionite concentration resulted in a hyposulfite ion binding in the active site.

The structure of PPG-inactivated PutA86−630 also implicates Arg431 in functional switching. In the THFA complex, Arg431 is poised above the hydride acceptor of the FAD and is thus positioned to sense the redox state of the flavin. The PPG-inactivated enzyme structure implies that reduction induces rupture of the N(5)−Arg431 hydrogen bond. This result is satisfying because it provides an explanation for previously reported results showing that replacement of Arg431 with Met or reconstitution of PutA with 5-deaza-FAD eliminated reductive activation of PutA−membrane binding (*7*). It was suggested at that time that Arg431 plays an important role in transmitting redox signals out of the PRODH active site that lead to activation of membrane binding and transcription of the *put* regulon, although the structure of the dithionite-reduced enzyme did not indicate any change in this residue. The structure reported here confirms the importance of Arg431 in functional switching and suggests that rupture of the N(5)−Arg431 hydrogen bond might be among the early events that occur in transmitting the membrane association signal from the flavin to the membrane-binding domain.

The PPG-inactivated enzyme structure suggests that Asp370 might also have a role in functional switching. The structure shows that flavin reduction weakens the interaction between Asp370 and Arg431, allowing the former residue to sample two side chain conformational states that are related by a rotation of 180° around χ_1. This result suggests the new hypothesis that transmission of the functional switching signal out of the active site involves correlated movement of Asp370 and Arg431.

Finally, the structure of the PPG-inactivated enzyme is unique among PutA PRODH domain structures in that helix 8 is substantially unfolded, the conserved Arg555−Glu289 ion pair is broken, and the β1−αl loop is withdrawn from the active site. Consequently, the active site is partially disassembled, and the *si* face of the isoalloxazine ring, i.e., the proline binding site, is exposed to solvent. We suggest that the disassembled active site reflects the absence of a bound proline analogue, rather than the reduced state of the flavin, because α8 and the β1−αl loop are critical for substrate binding. In particular, Tyr552, Arg555, and Arg556 of α8 directly contact the substrate, Glu559 of α8 stabilizes Arg556 through ion pairing, and Glu289 of the β1−αl loop ion pairs with Arg555 (Figure 9). Furthermore, the open active site of the PPG-inactivated enzyme bears a striking resemblance to that of oxidized TtPRODH, the only other PRODH structure with an empty proline binding site (Figure 10).

We thus suggest that the collective structural information about the PutA PRODH domain and TtPRODH provides clues about conformational changes attendant to substrate binding. The structures imply that the active site might be incompletely assembled in the absence of the substrate, and the binding of proline stabilizes residues of α8 and draws the β1−αl loop into the active site to connect the loop with α8 via the conserved ion pair. In this scenario, the ion pair might function as a gate that closes and opens in response to substrate binding and product release, respectively. Further experiments are needed to test these ideas. In this regard, structures of the ligand-free, oxidized PutA PRODH domain and a monofunctional PRODH in a complex with THFA would be especially enlightening.

ACKNOWLEDGMENT

We thank Dr. Jay Nix of Advanced Light Source beamline 4.2.2 for help with data collection. The Advanced Light Source is supported by the Director, Office of Science, Office of Basic Energy Sciences, of the U.S. Department of Energy under Contract DE-AC02-05CH11231.

REFERENCES

1. Zhou, Y., Zhu, W., Bellur, P. S., Rewinkel, D., and Becker, D. F. (2008) Direct linking of metabolism and gene expression in the proline utilization A protein from *Escherichia coli*. *Amino Acids 35*, 711–718.
2. Tanner, J. J. (2008) Structural biology of proline catabolism. *Amino Acids 35*, 719–730.
3. Zhou, Y., Larson, J. D., Bottoms, C. A., Arturo, E. C., Henzl, M. T., Jenkins, J. L., Nix, J. C., Becker, D. F., and Tanner, J. J. (2008) Structural basis of the transcriptional regulation of the proline utilization regulon by multifunctional PutA. *J. Mol. Biol. 381*, 174–188.
4. Abrahamson, J. L., Baker, L. G., Stephenson, J. T., and Wood, J. M. (1983) Proline dehydrogenase from *Escherichia coli* K12. Properties of the membrane-associated enzyme. *Eur. J. Biochem. 134*, 77–82.
5. Brown, E. D., and Wood, J. M. (1992) Redesigned purification yields a fully functional PutA protein dimer from *Escherichia coli*. *J. Biol. Chem. 267*, 13086–13092.
6. Menzel, R., and Roth, J. (1981) Enzymatic properties of the purified putA protein from *Salmonella typhimurium*. *J. Biol. Chem. 256*, 9762–9766.

7. Zhang, W., Zhang, M., Zhu, W., Zhou, Y., Wanduragala, S., Rewinkel, D., Tanner, J. J., and Becker, D. F. (2007) Redox-induced changes in flavin structure and roles of flavin N(5) and the ribityl 2′-OH group in regulating PutA-membrane binding. *Biochemistry 46*, 483–491.
8. Zhang, W., Zhou, Y., and Becker, D. F. (2004) Regulation of PutA-membrane associations by flavin adenine dinucleotide reduction. *Biochemistry 43*, 13165–13174.
9. Wood, J. M. (1987) Membrane association of proline dehydrogenase in *Escherichia coli* is redox dependent. *Proc. Natl. Acad. Sci. U.S.A. 84*, 373–377.
10. White, T. A., Johnson, W. H., Jr., Whitman, C. P., and Tanner, J. J. (2008) Structural basis for the inactivation of *Thermus thermophilus* proline dehydrogenase by N-propargylglycine. *Biochemistry 47*, 5573–5580.
11. Zhu, W., and Becker, D. F. (2005) Exploring the proline-dependent conformational change in the multifunctional PutA flavoprotein by tryptophan fluorescence spectroscopy. *Biochemistry 44*, 12297–12306.
12. Ostrander, E. L., Larson, J. D., Schuermann, J. P., and Tanner, J. J. (2009) A conserved active site tyrosine residue of proline dehydrogenase helps enforce the preference for proline over hydroxyproline as the substrate. *Biochemistry 48*, 951–959.
13. Leslie, A. G. (2006) The integration of macromolecular diffraction data. *Acta Crystallogr. D62*, 48–57.
14. Evans, P. (2006) Scaling and assessment of data quality. *Acta Crystallogr. D62*, 72–82.
15. Potterton, E., Briggs, P., Turkenburg, M., and Dodson, E. (2003) A graphical user interface to the CCP4 program suite. *Acta Crystallogr. D59*, 1131–1137.
16. Matthews, B. W. (1968) Solvent content of protein crystals. *J. Mol. Biol. 33*, 491–497.
17. Nadaraia, S., Lee, Y. H., Becker, D. F., and Tanner, J. J. (2001) Crystallization and preliminary crystallographic analysis of the proline dehydrogenase domain of the multifunctional PutA flavoprotein from *Escherichia coli*. *Acta Crystallogr. D57*, 1925–1927.
18. Lee, Y. H., Nadaraia, S., Gu, D., Becker, D. F., and Tanner, J. J. (2003) Structure of the proline dehydrogenase domain of the multifunctional PutA flavoprotein. *Nat. Struct. Biol. 10*, 109–114.
19. Zhang, M., White, T. A., Schuermann, J. P., Baban, B. A., Becker, D. F., and Tanner, J. J. (2004) Structures of the *Escherichia coli* PutA proline dehydrogenase domain in complex with competitive inhibitors. *Biochemistry 43*, 12539–12548.
20. Vagin, A., and Teplyakov, A. (2000) An approach to multi-copy search in molecular replacement. *Acta Crystallogr. D56* (Part 12), 1622–1624.
21. Zwart, P. H., Afonine, P. V., Grosse-Kunstleve, R. W., Hung, L. W., Ioerger, T. R., McCoy, A. J., McKee, E., Moriarty, N. W., Read, R. J., Sacchettini, J. C., Sauter, N. K., Storoni, L. C., Terwilliger, T. C., and Adams, P. D. (2008) Automated structure solution with the PHENIX suite. *Methods Mol. Biol. 426*, 419–435.
22. Emsley, P., and Cowtan, K. (2004) Coot: Model-building tools for molecular graphics. *Acta Crystallogr. D60*, 2126–2132.
23. Macheroux, P. (1999) UV-Visible Spectroscopy as a Tool to Study Flavoproteins. In *Flavoprotein Protocols* (Chapman, S. K., and Reid, G. A., Eds.) pp 1−7, Humana Press, Totowa, NJ.
24. Kitz, R., and Wilson, I. B. (1962) Esters of methanesulfonic acid as irreversible inhibitors of acetylcholinesterase. *J. Biol. Chem. 237*, 3245–3249.
25. Silverman, R. B. (1995) Mechanism-based enzyme inactivators. *Methods Enzymol. 249*, 240–283.
26. Zhu, W., and Becker, D. F. (2003) Flavin redox state triggers conformational changes in the PutA protein from *Escherichia coli*. *Biochemistry 42*, 5469–5477.
27. Brown, E. D., and Wood, J. M. (1993) Conformational change and membrane association of the PutA protein are coincident with reduction of its FAD cofactor by proline. *J. Biol. Chem. 268*, 8972–8979.
28. White, T. A., Krishnan, N., Becker, D. F., and Tanner, J. J. (2007) Structure and kinetics of monofunctional proline dehydrogenase from *Thermus thermophilus*. *J. Biol. Chem. 282*, 14316–14327.
29. Tritsch, D., Mawlawi, H., and Biellmann, J. F. (1993) Mechanism-based inhibition of proline dehydrogenase by proline analogues. *Biochim. Biophys. Acta 1202*, 77–81.
30. Engh, R. A., and Huber, R. (1991) Accurate bond and angle parameters for X-ray protein structure refinement. *Acta Crystallogr. A47*, 392–400.
31. Lovell, S. C., Davis, I. W., Arendall, W. B., III, de Bakker, P. I., Word, J. M., Prisant, M. G., Richardson, J. S., and Richardson, D. C. (2003) Structure validation by Cα geometry: ϕ, ψ and Cβ deviation. *Proteins 50*, 437–450.